Experimental and *ab-initio* calculated vcd spectra of the first OH-stretching overtone of (1*R*)-(−) and (1*S*)-(+)-*endo*-BORNEOL

Fabrizio Gangemi,[ab] Roberto Gangemi,[ab] Giovanna Longhi[ab] and Sergio Abbate*[ab]

Received 17th October 2008, Accepted 8th January 2009
First published as an Advance Article on the web 24th February 2009
DOI: 10.1039/b818432a

The near infrared (NIR) absorption and NIR-vibrational circular dichroism (NIR-VCD) spectra of dilute solutions of the two enantiomers of *endo*-borneol have been measured in the first OH-stretching overtone region (1600–1300 nm). By density functional theory (DFT) we calculate mechanical parameters, *i.e.* the harmonic mechanical frequency and the anharmonicity constant for the OH stretching, and anharmonic electrical parameters; *i.e.* the dependence on OH-bond length of atomic polar tensors and atomic axial tensors. We evaluate transition integrals for the calculations of rotational and dipole strengths by Morse anharmonic wavefunctions depending on mechanical harmonic frequencies and mechanical anharmonicity parameters that are calculated *ab initio*. Experimental and calculated spectra compare quite well and this fact allows us to associate differently signed NIR-VCD features with different conformational states of the OH-bond. Absorption features for the fundamental and for the second overtone of the OH stretching are also compared with experiment.

1. Introduction

Traditional spectroscopic studies, including infrared spectroscopy (IR)[1] and vibrational circular dichroism[2–5] (VCD), in case of chiral molecules containing hydroxyl groups can give important information concerning molecular conformation and possible inter- and intra-molecular hydrogen bonding. Experimental data become more informative if supported by reliable *ab initio* methods to calculate spectra. As far as VCD is concerned, for reasons tied both to experimental and theoretical difficulties, there has been a tendency in past years to privilege the mid-IR region rather than the OH-stretching region, even though recently one may record some renewed attention to the OH-stretching data.[5,6] One difficulty in interpreting IR-VCD data of alcohols is also the large number of conformations even for small molecules such as *n*-butanol.[7–9] We wish to treat here the case of borneol or, in general, of alcohols related to bicyclic structures like, *e.g.*, fenchyl alcohol. For these molecules the only non rigid moiety is the OH bond itself, which may rotate around the CO bond; this mobility has consequences on all spectroscopic regions of a VCD spectrum, even in the mid-IR, as pointed out by Devlin *et al.*[10] To make sure that the comparison of VCD experimental and calculated spectra is sensible, one has to deal with quite dilute solutions. We have checked from IR spectra in the fundamental OH-stretching region (3000–3800 cm^{-1}) that 0.06 M borneol solutions in CCl_4 may serve our purposes.[10]

In this study we report the experimental near infrared (NIR)-VCD spectra for the first overtone region, $\Delta v = 2$, (1600–1300 nm) of the two enantiomers of *endo*-borneol at the aforementioned concentration and we carry out their interpretation through a method that we have recently devised[11], based on *ab initio* calculations.

In absorption spectroscopy the NIR region has received through the years a lot of attention[1,2] and recently the OH overtone spectra have been examined by 2D-NIR investigations,[12,13] and by laser-intracavity photoacoustic studies[14,15] with ancillary *ab initio* based theoretical interpretations. Our study may be placed in the same category as those of ref. 14 and 15, except that it deals with chiral molecules and it presents for the first time the calculation of magnetic dipole moment derivatives at higher order in addition to corresponding electric dipole moment derivatives. The method of ref. 11 is derived starting from the studies of Bak *et al.*,[16] who first included anharmonic effects within *ab initio* calculations of IR-VCD spectra. We wish to point out that in ref. 11, the application of theory to the evaluation of camphor and camphorquinone NIR-VCD spectra had two shortcomings, that will not appear here. First, an explicit hypothesis was made that the sixteen (or fourteen) CH-stretching modes are local at $\Delta v \geq 3$ (v = vibrational level order − 1); secondly the mechanical anharmonicity parameters were not evaluated *ab initio*, but transferred from previous absorption experiments. In the present case the local character of the vibrational mode is a fact, since only one OH bond is present in the molecule. Also we have run the calculation of the anharmonicity parameter *ab initio*. For both these reasons the present work does not contain any empirical parameter whatsoever and provides, to our knowledge, the first full *ab initio* calculation of an overtone VCD spectrum. As recalled above, of course the OH bond may

[a] *Dipartimento di Scienze Biomediche e Biotecnologie, Viale Europa 11, 25123 Brescia, Italy. E-mail: abbate@med.unibs.it; Fax: +39 030 371 7416; Tel: +39 030 371 7415*
[b] *Consorzio Nazionale Interuniversitario per le Scienze Fisiche della Materia, Via della Vasca Navale, 84, 00146 Roma, Italy*

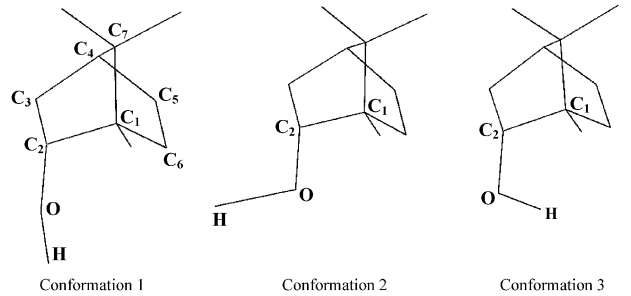

Fig. 1 Representation of the three stable conformers of (1*S*)-*endo*-borneol, as predicted by DFT calculations (for more details see text). Hydrogen atoms not reported except for the OH bond (see also Table 1 for numbering and precise characteristics).

rotate around the CO bond in an otherwise rigid structure. From the use of the GAUSSIAN *ab initio* package[17] (DFT method with functional and basis set described later) we indeed find three minimum-energy conformational states that we report in Fig. 1 and we will discuss them in more detail later. For each one of the three structures in Fig. 1 we have applied our *ab initio* method.

2. Method, results and discussion

In Fig. 2 we give the experimental NIR and NIR-VCD spectra of the two enantiomers (1*S*)-(+)-*endo*-borneol and (1*R*)-(−)-*endo*-borneol in 0.06 M/CCl_4 solutions, recorded with the home-made apparatus described earlier.[18,19] The spectra were taken in 5 cm-pathlength quartz cuvettes and are the results of 10–30 accumulations, in sequences of smaller sets of spectra (2 or 3 each), as described in ref. 19. The VCD spectra for the two enantiomers are mirror images, as they should be, and the signal-to-noise ratio is acceptable, given also that this region is not the best accessible one to our instrument.

The choice of studying the first overtone region of the OH-stretching is due to optimal performance of dispersive instruments in that range. VCD data in the fundamental OH stretching region are not so much discussed in the literature, the next overtone region ($\Delta v = 3$) presents the inconvenience that one needs too much compound, in order to fill a longer pathlength cell, even though one may expect an improved resolution of OH-overtone signals due to increased separation thereof, as prescribed by the Birge–Sponer law (*vide infra*) at higher v. In any case we have not tried that region yet. However, the advantages in the study of the overtones' range are not only due to the efficiency of our apparatus; there are some practical advantages of the NIR-VCD technique, as pointed out by Nafie *et al.*[20] or Sugeta,[21] and also some more fundamental reasons for choosing the NIR region, as recalled by Sandorfy.[22] Indeed, unlike the fundamental absorption region, the first overtone of the OH-stretching is more intense for the free OH group than for the H-bonded one.

To interpret the data of Fig. 2, we make use here of the algorithm that we had developed in ref. 11, and further extend here, so as to make our method fully *ab initio*. The electric

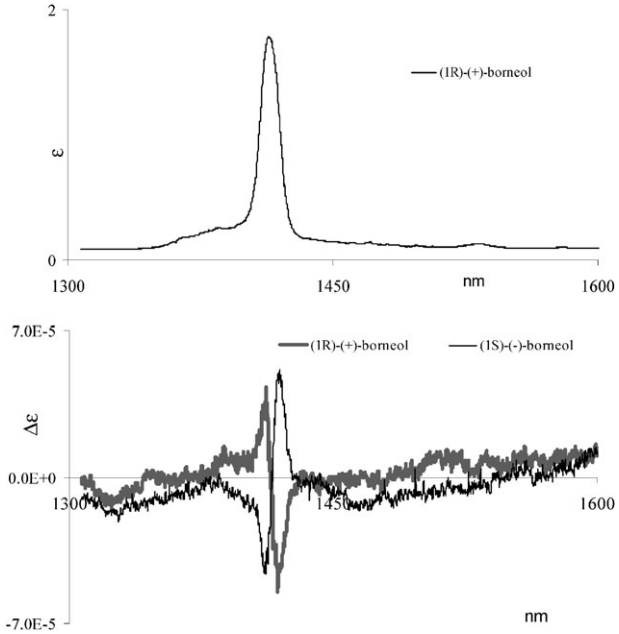

Fig. 2 Experimental NIR absorption of (1*R*)-(−)-*endo*-borneol (top panel) ($\Delta v = 2$) and superimposed NIR-VCD spectra of (1*R*)-(−)-*endo*-borneol and (1*S*)-(+)-*endo*-borneol (bottom panel) ($\Delta v = 2$) for 0.06 M CCl_4 solutions; for other experimental conditions see text.

dipole transition moment $\langle \mu_i \rangle_{0v}$ and magnetic dipole transition moment $\langle m_i \rangle_{0v}$ for the vibrational transition $0 \rightarrow v$ are given by:

$$\langle \mu_i \rangle_{0v} = \sum_{\alpha j} \Pi^0_{\alpha ij} \frac{L^n_{\alpha j}}{\sqrt{m_G}} \langle 0|Q_n|v\rangle + \frac{1}{2}\sum_{\alpha j \beta k} \left(\frac{\partial \Pi_{\alpha ij}}{\partial R_{\beta k}}\right)_0 \frac{L^n_{\alpha j} L^n_{\beta k}}{m_G} \langle 0|Q_n^2|v\rangle + \frac{1}{6}\sum_{\alpha j \beta k \gamma l} \left(\frac{\partial^2 \Pi_{\alpha ij}}{\partial R_{\beta k} \partial R_{\gamma l}}\right)_0 \frac{L^n_{\alpha j} L^n_{\beta k} L^n_{\gamma l}}{(m_G)^{3/2}} \langle 0|Q_n^3|v\rangle + \cdots \quad (1)$$

$$\langle m_i \rangle_{v0} = 2\hbar \sum_{\alpha j} A^0_{\alpha ij} \frac{L^n_{\alpha j}}{\sqrt{m_G}} \langle v|P_n|0\rangle + 2\hbar \sum_{\alpha j}\sum_{\beta k} \left(\frac{\partial A_{\alpha ij}}{\partial R_{\beta k}}\right)_0 \frac{L^n_{\alpha j} L^n_{\beta k}}{m_G} \langle v|Q_n P_n|0\rangle + \frac{1}{2}\hbar \sum_{\alpha j \beta k \gamma l} \left(\frac{\partial^2 A_{\alpha ij}}{\partial R_{\beta k} \partial R_{\gamma l}}\right)_0 \frac{L^n_{\alpha j} L^n_{\beta k} L^n_{\gamma l}}{(m_G)^{3/2}} \times (\langle v|Q_n^2 P_n|0\rangle - \langle 0|Q_n^2 P_n|v\rangle) + \cdots \quad (2)$$

where the atomic polar tensors (APT), $\Pi_{\alpha ij}$, and the atomic axial tensors (AAT),[23,16] $A_{\alpha ij}$, are expanded as functions of the Cartesian coordinates $R_{\beta k}$ of nuclei; Q_n and P_n are the normal (or local) coordinate for mode n and its conjugate momentum, respectively; the set of coefficients $L^n_{\alpha j}$ may be interpreted as the normalized Cartesian displacements of the α-nucleus along the Cartesian axis j, corresponding to the vibrational mode n, and the mass factors m_G are related to their normalization; and,

finally, $\hbar = h/2\pi$ is the reduced Planck's constant. Similar equations were presented by Bak *et al.*[16] in the normal mode approach to treat anharmonicity corrections in mid-IR VCD calculations. For a local stretching mode, as is the case of the OH stretching mode studied in this work, eqn (1) and (2) may be transformed to[11]

$$\begin{aligned}\langle \mu_i \rangle_{0v} = &\sum_{\alpha=\mathrm{H,O}} \Pi^0_{\alpha i3} L^n_{\alpha 3} \sqrt{\frac{m_\mathrm{R}}{m_\mathrm{G}}} \langle 0|z - z_\mathrm{e}|v\rangle \\ &+ \frac{1}{2} \sum_{\alpha=\mathrm{H,O}} \left(\frac{\partial \Pi_{\alpha i3}}{\partial z}\right)_0 L^n_{\alpha 3} \sqrt{\frac{m_\mathrm{R}}{m_\mathrm{G}}} \langle 0|(z - z_\mathrm{e})^2|v\rangle \\ &+ \frac{1}{6} \sum_{\alpha=\mathrm{H,O}} \left(\frac{\partial^2 \Pi_{\alpha i3}}{\partial z^2}\right)_0 L^n_{\alpha 3} \sqrt{\frac{m_\mathrm{R}}{m_\mathrm{G}}} \langle 0|(z - z_\mathrm{e})^3|v\rangle + \cdots \end{aligned} \tag{3}$$

$$\begin{aligned}\langle m_i \rangle_{v0} = &2\hbar \sum_{\alpha=\mathrm{H,O}} A^0_{\alpha i3} \frac{L^n_{\alpha 3}}{\sqrt{m_\mathrm{R} m_\mathrm{G}}} \langle v|p|0\rangle \\ &+ 2\hbar \sum_{\alpha=\mathrm{H,O}} \left(\frac{\partial A_{\alpha i3}}{\partial z}\right)_0 \frac{L^n_{\alpha 3}}{\sqrt{m_\mathrm{R} m_\mathrm{G}}} \langle v|(z - z_\mathrm{e})p|0\rangle \\ &+ \frac{1}{2}\hbar \sum_{\alpha=\mathrm{H,O}} \left(\frac{\partial^2 A_{\alpha i3}}{\partial z^2}\right)_0 \frac{L^n_{\alpha 3}}{\sqrt{m_\mathrm{R} m_\mathrm{G}}} \\ &\times (\langle v|(z - z_\mathrm{e})^2 p|0\rangle - \langle 0|(z - z_\mathrm{e})^2 p|v\rangle) + \cdots \end{aligned} \tag{4}$$

where z is the internal OH stretching coordinate, with equilibrium value z_e, p is its canonical conjugate, $m_\mathrm{R} = M_\mathrm{H}M_\mathrm{O}/M_\mathrm{OH}$ is the OH reduced mass, and the only relevant $L^n_{\alpha j}$ coefficients are those with $j = 3$, because the z axis is chosen along the OH bond. A great simplification is thus achieved since, in place of the mixed derivatives appearing in eqn (1) and (2), one has to evaluate derivatives with respect to the single internal stretching coordinate: these derivatives are easily obtained by polynomial interpolation of DFT calculated APT and AAT values on a one-dimensional grid of points.[11]

The transition moments in eqn (1) and (2) are evaluated from Morse potential wavefunctions.[11] For the calculation of frequency ω_v at overtone order $v - 1$, the Morse formula for eigenvalues is adopted,

$$\omega_v = \omega_0 \left(v + \frac{1}{2}\right) - \chi \left(v + \frac{1}{2}\right)^2 \tag{5}$$

The mechanical frequency ω_0 is taken from the harmonic calculations as implemented in GAUSSIAN03[17] at the DFT level. Its values for the three conformers of borneol are shown in Table 1. The parameter χ is worked out by an *ab initio* determination of the potential energy curve U of the molecule *versus* the internal stretching coordinate, and this is where the procedure presented in this work is an extension of that of ref. 11. The curve is obtained as a polynomial fitting to a set of points at which the potential energy is evaluated *ab initio*. It is well known that a potential with cubic and quartic terms gives the same eigenvalues as in eqn (5) with second order perturbative treatment if the following relation between χ and potential derivatives holds:[24]

$$\chi = \frac{h}{64\pi^2 mc} \left(\frac{5}{3}\frac{K_3^2}{K_2^2} - \frac{K_4}{K_2}\right), \tag{6}$$

where $K_j = \frac{\partial^j U}{\partial q^j}$, q is the internal stretching coordinate $q = (z - z_\mathrm{e})$ (here the OH bond length), m is the reduced mass of the OH oscillator, and c is the velocity of light. This formula, when using a polynomial fitting of the potential, gives a good estimate[14,15] of χ, and is therefore adopted here. For each one of the three OH conformations in (1*S*)-*endo*-borneol (*vide infra*) 25 equally spaced points are examined in the q-coordinate range [−0.3 Å, 0.3 Å] around equilibrium by *ab initio* DFT calculations at B3LYP/6-31G** level. Such functional/basis choice is known to give good accuracy for VCD,[19b] with a computational effort compatible with the number of grid points considered in this procedure. Various polynomial interpolations have been considered with polynomial degrees from 4 to 20. A study of uncertainties annexed to the fitting procedure indicates that the coefficients entering into the determination of χ (2nd, 3rd and 4th derivatives of potential energy) are most accurately known at degrees 7 to 9. An average of the values obtained with these three polynomial expansions, weighted with statistical errors, is then adopted in this work. We have verified that our method works pretty well for ethylene glycol, for which independent calculations with various basis sets and good experimental data exist,[14] with agreement within 2–3 cm^{-1}. We prefer to follow this procedure to calculate the mechanical anharmonicity of the OH–bond, rather than using the GAUSSIAN algorithm[17] developed by Barone,[25] not only due to the success reported in the literature for this method,[14] but also because it is less heavy from a computational viewpoint since it refers to a really local property. The procedure adopted here disregards cubic and quartic cross terms involving other normal modes: this simplifies the calculation, which otherwise would require displacements along all 81 normal modes, permitting in less time a precise evaluation of the diagonal anharmonicity constant.

Also, the value for ω_0 could be obtained by the same polynomial interpolation as used for the calculations of χ. In this way we obtain $\omega_0(1) = 3814.4$, $\omega_0(2) = 3831.3$, $\omega_0(3) = 3825.5$ cm^{-1}, for the three conformations of Table 1. These values come from an actual local mode and are slightly higher than the corresponding ones in Table 1, which come from a harmonic normal mode, where other

Table 1 Calculated mechanical and electrical harmonic and anharmonic parameters for (1*S*)-*endo*-borneol in its three conformational states. Population percentages calculated on the basis of ΔG at 298 K

Conformation #	$\tau^\circ(\mathrm{HOC_2C_1})$	ΔG/kcal mol^{-1}	Population (%)	$\omega_0/\mathrm{cm}^{-1}$	χ/cm^{-1}	$(\partial\mu z/\partial q)$/e	$(\partial^2\mu/\partial q^2)$/e $\mathrm{Å}^{-1}$
1	68	0	51.5	3807	88.6	0.080	−0.629
2	174	0.35	28.3	3822	86.8	0.103	−0.736
3	300	0.55	20.2	3814	90.0	0.062	−0.446

atoms are weakly involved in the vibration. The two sets of ω_0-values provide quite similar results.

The application of the method outlined above to (1*S*)-camphor and (1*S*)-camphorquinone in ref. 11, where χ had been taken from experiments, provided an excellent interpretation of the overtone VCD data at $\Delta v = 3$. However it had two shortcomings: (a) the assumption of local modes: in molecules like Camphor one cannot exclude that harmonic and anharmonic couplings lead possibly to residual normal modes; (b) in eqn (2) terms in p^3 may not be excluded.[26] None of these limitations is present in the borneol case, where the OH-stretching can safely be considered a local mode and we need just to stop at second order in eqn (1) and (2), since we are mainly interested in the first overtone transitions $\Delta v = 2$. One has rather to take into account the three conformations of the OH-bond in borneol, which are independent of each other, and construct the result as a thermodynamic average over them.

The DFT conformational analysis of (1*S*)-*endo*-borneol at the B3LYP/6-31G** level gives three geometries with comparable energies, corresponding to three different positions of the OH-bond with respect to the rest of the molecule. The values for selected parameters describing their geometrical, dynamical, and electrical properties are reported in Table 1. The nomenclature for the carbon atoms is the standard one for camphor-like molecules (C_2 being the closest carbon atom to the OH bond and C_1 the closest stereogenic carbon atom). The data are reported in order of increasing free energy, and energy as well, and thus in decreasing order of population. The calculated values of ω_0 and χ may be compared with the experimental values derived by a Birge–Sponer plot based on our own solution absorption spectra at $\Delta v = 1$, 2, and 3. We have $\omega_0^{\exp} = 3796 \pm 3\ \mathrm{cm}^{-1}$ and $\chi = 86 \pm 2\ \mathrm{cm}^{-1}$ where, due to the low resolution of the spectra recorded in the liquid phase, we just considered the central wavenumber or wavelength of the absorption bands.

Let us now consider the results of the calculation for the derivatives of APT and AATs up to second order, with adequate choice of the *z*-coordinate and with full consideration of both oxygen and hydrogen atoms' APTs and AATs and derivatives, as explained in ref. 11. Differently from the calculations of ω_0 and χ, the H-displacement in the OH stretching here is [−0.4 Å, 0.4 Å], with a step of 0.08 Å; the O-displacement is defined accordingly. To appreciate the results we report in Fig. 3 the *xz*, *yz*, and *zz* components of APT and AAT tensors for the H atom involved in the OH bond as functions of the OH-stretching coordinate: the *z*-axis is chosen along the OH bond from O to H (and the *z*-coordinate is related to the internal coordinate q through: $q = z_H - z_O$), y is on the HOC_2 plane and x is perpendicular to it so as to form a right-handed system with y and z. Considering APTs and AATs for the H atom is instructive and allows us to rationalize the results for the calculated spectra. We must say however that the contribution of the O atom is also important[11] and of course we have included it in the present calculations. From Table 1 we observe that $\mathrm{APT}_{zz}(0) = (\partial\mu_z/\partial q)_0$ is positive for all conformers of OH, as opposite to the CH case. We obtain also that $(\partial \mathrm{APT}_{zz}/\partial q)_0 = (\partial^2\mu_z/\partial q^2)_0$ is negative, like the CH case, for all conformers of OH. We obtain sizeable values for the transverse components x and y of the second derivatives of μ, unlike the CH case. The trend in AAT values and their derivatives calculated for OH bonds is similar to that predicted for CH bonds, *i.e.* high transverse components and low longitudinal components. Interestingly, for the most populated conformer #1, defined by $\tau(HOC_1C_2) = 68°$, the behaviour of

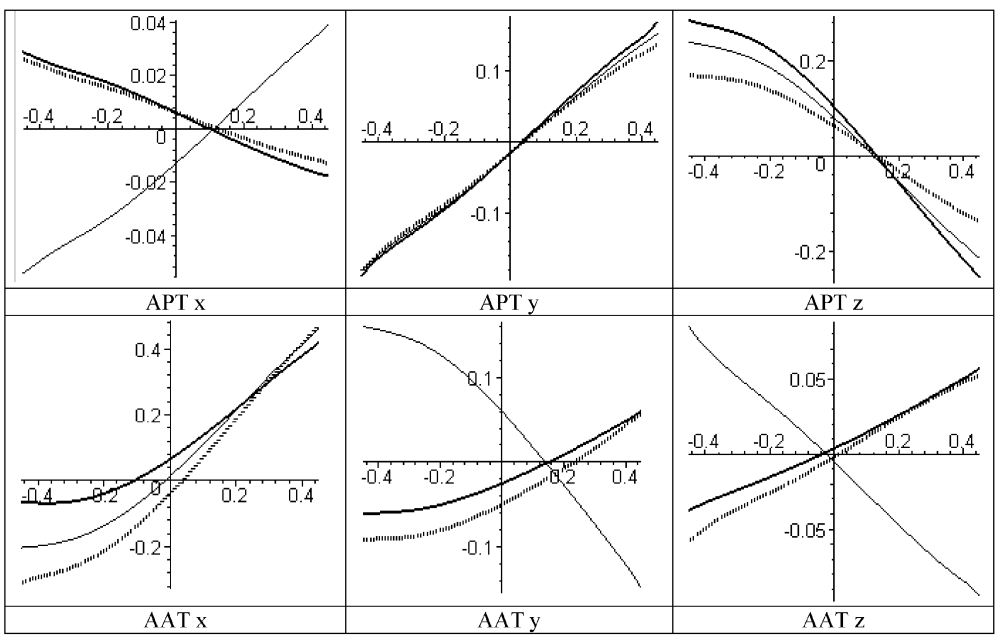

Fig. 3 Dependence from the OH stretching coordinate of the components APT_{iz} and AAT_{iz} ($i = x, y, z$) for the H-atom of OH in the three conformations of (1*S*)-*endo*-borneol. Horizontal axes units: Å. Vertical axes units: e (electron charge) for APTs and ($ea_0/\hbar c$) for AATs (a_0 Bohr radius, $\hbar$ reduced Planck's constant, c speed of light). Conformer #1: thin solid line; conformer #2: medium dash line; conformer #3: thick dot line (see Table 1).

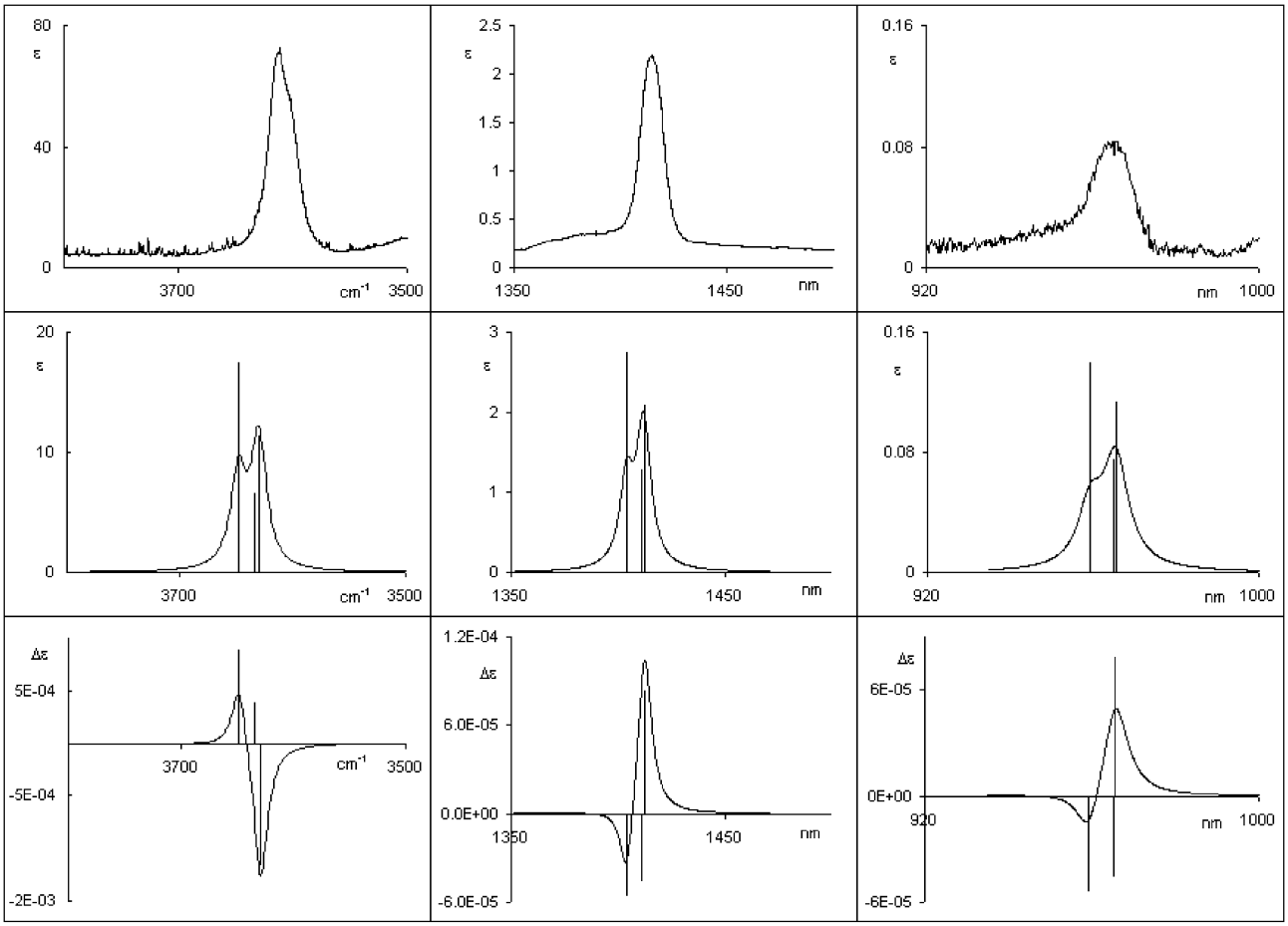

Fig. 4 Experimental IR and NIR absorption spectra for (1*S*)-*endo*-borneol (top row) compared to the corresponding calculated spectra (middle row). We report the calculated IR- and NIR-VCD spectra in the lowest row. Spectra of the three conformers are summed with Boltzmann statistical weights based on ΔG. ε and $\Delta\varepsilon$ are in 10^3 cm^2 mol^{-1} units. Bars for the calculated transitions proportional to dipole strengths and rotational strengths are also reported in arbitrary units.

components APT_{xz}, AAT_{yz} and AAT_{zz} as functions of q is opposite to that of the other two conformers. This is relevant for the explanation of the different sign of the rotational strength of this conformer with respect to the other two, as explained below. In Fig. 4 we report the calculated absorption and VCD spectra for $\Delta v = 1$, 2, and 3 and the corresponding experimental absorption spectra. The calculated spectra have been obtained by determining the transition moments as described in eqn (3) and (4) with corrections up to the appropriate order of the dipole expansion (first order for $\Delta v = 1$, second order for $\Delta v = 2$ and third order for $\Delta v = 3$) and by assigning Lorentzian band shapes to dipole and rotational strengths, with bandwidths of 8 cm^{-1} for $\Delta v = 1$, 20 cm^{-1} ($\approx$5nm) for $\Delta v = 2$, and 40 cm^{-1} ($\approx$ 7 nm) for $\Delta v = 3$. Spectra for the three conformers were weighted with the population factors of Table 1. The experimental absorption spectra compare nicely with our calculations and this is not unexpected; Kjaergaard *et al*[14,15] had already shown that the method expounded here provides good results. The calculated VCD spectra exhibit an interesting inversion from $\Delta v = 1$ (IR) to $\Delta v = 2$, and $\Delta v = 3$ (NIR). The reason for this behavior may be traced in Fig. 3. One may see that the signs of bands in $\Delta v = 1$ spectra are mainly determined by the y components of APT and AAT at equilibrium. For conformer #1 $APT_{yz}(0) < 0$ and $AAT_{yz}(0) > 0$ giving a negative cross product, as of the definition of rotational strength; on the opposite hand $APT_{yz}(0) < 0$ and $AAT_{yz}(0) < 0$ for conformers 2 and 3. Instead the NIR-VCD spectrum at $\Delta v = 2$ is determined by the second order terms in eqn (3) and (4), while first order terms give negligible contributions. Thus the different signs of the bands essentially depend on the first derivatives of APT and AAT components with respect to q: as can be seen in Fig. 3, when an APT component for conformer 1 has the same slope as the other two conformers, the same AAT component has opposite slope, and *vice versa*, so that a rotational strength of opposite sign is obtained for conformer 1 with respect to conformers 2 and 3. For $\Delta v = 3$ one has similar results to $\Delta v = 2$ since higher derivatives of APT and AAT are small.

Finally in Fig. 5 we compare experimental and calculated NIR-VCD spectra at $\Delta v = 2$, for which we have VCD data; we report the calculated results already given in Fig. 4 as well as those obtained assigning equal statistical weights to the three conformers (the latter population factors are more in line with those indicated by higher order basis sets calculations by Devlin *et al.*[10]). The results are quite encouraging, the

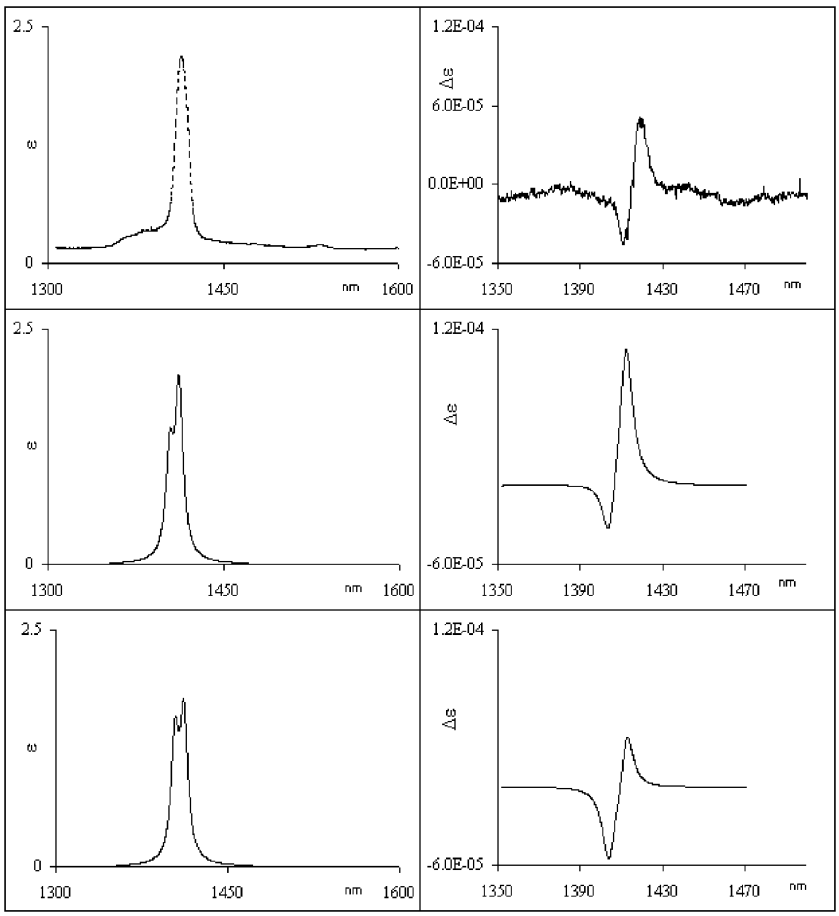

Fig. 5 Comparison of experimental (Top) and calculated NIR (left) NIR-VCD (right) spectra of (1*S*)-(+)-*endo*-borneol at $\Delta v = 2$. Results of the calculations in the middle row obtained from averages with statistical weights based on ΔG; results in the bottom row obtained by arithmetic averages over three conformers. Assumed $\Delta\lambda = 5$ nm; ε and $\Delta\varepsilon$ are in 10^3 cm^2 mol^{-1} units.

prediction of both NIR and NIR-VCD spectra being almost as of experiments in terms of signs (for VCD), band positions and band intensities. We wish to emphasize that the present calculation has been conducted fully *ab initio*, only the choice of Lorentzian band-width is empirical, as done in all VCD literature in the IR case.

3. Conclusions

In this work, for the first time, we have carried out a full *ab initio* calculations of $\Delta v = 2$ OH stretching VCD spectra and have found a very good correspondence between experiment and calculations. Of course (1*S*)-borneol, like all alcohols containing one OH, is treatable on the basis of the present approach, since there is no doubt here that modes are local. For molecules containing more than one OH (or in general XH), the approach should be generalized. The only complication here is due to the presence of multiple conformations for the OH bond. However this fact reveals an advantage of this study since this technique generates hopes of directly "measuring" the conformations of a very mobile moiety like the OH bond, in dilute or even more concentrated solutions. In the latter respect we report that preliminary results on 1 M (1*S*)-borneol solutions have been obtained in the region of the 1st overtone OH-stretching: the VCD signal attributed to the "free" OH-stretchings is still present and usable, analogously to what has been proposed on the basis of 2D-NIR absorption spectroscopy.[13] Finally we wish to report that good results have been also obtained in other simple chiral alcohols like (1*R*)-fenchyl alcohol.

References

1 G. C. Pimentel and A. L. McClellan, *The Hydrogen Bond*, W.H. Freeman, S. Francisco, 1968.
2 C. Marcott, C. C. Blackburn, T. R. Faulkner and A. Moscowitz, *J. Am. Chem. Soc.*, 1978, **100**, 5262.
3 T. A. Keiderling and P. J. Stephens, *J. Am. Chem. Soc.*, 1977, **99**, 8061.
4 T. B. Freedman, G. A. Balukjian and L. A. Nafie, *J. Am. Chem. Soc.*, 1985, **107**, 6213–622.
5 P. L. Polavarapu, C. S. Ewig and T. Chandramouly, *J. Am. Chem. Soc.*, 1987, **109**, 7382–7386.
6 T. Buffeteau, L. Ducasse, A. Brizard, I. Huc and R. Oda, *J. Phys. Chem. A*, 2004, **108**, 4080–4086.
7 F. Wang, P. L. Polavarapu, F. Lebon, G. Longhi, S. Abbate and M. Catellani, *J. Phys. Chem. A*, 2002, **106**, 12365–12369.
8 F. Wang and P. L. Polavarapu, *J. Phys. Chem. A*, 2001, **105**, 6991–6997.
9 K. Yamamoto, Y. Nakao, Y. Kyogoku and H. Sugeta, *J. Mol. Struct. (THEOCHEM)*, 1991, **242**, 75–86.
10 F. J. Devlin, P. J. Stephens and P. Besse, *J. Org. Chem.*, 2005, **70**, 2980–2993.

11 F. Gangemi, R. Gangemi, G. Longhi and S. Abbate, *Vib. Spectrosc.*, 2009, DOI: 10.1016/j.vibspec.2009.01.004.
12 M. A. Czarnecki, H. Maeda, Y. Ozaki, M. Suzuki and M. Iwahashi, *J. Phys. Chem. A*, 1998, **102**, 9117–9123.
13 M.-A. Czarnecki, *J. Phys. Chem. A*, 2003, **107**, 1941–1944.
14 D. A. Howard, P. Jørgensen and H. G. Kjaergaard, *J. Am. Chem. Soc.*, 2005, **127**, 17096–17103.
15 D. A. Howard and H. G. Kjaergaard, *J. Phys. Chem. A*, 2006, **110**, 10245–10250.
16 K. L. Bak, O. Bludský and P. Jørgensen, *J. Chem. Phys.*, 1995, **103**(24), 10548–10555.
17 M. J. Frisch, G. W. Trucks, H. B. Schlegel, G. E. Scuseria, M. A. Robb, J. R. Cheeseman, J. A. Montgomery, Jr., T. Vreven, K. N. Kudin, J. C. Burant, J. M. Millam, S. S. Iyengar, J. Tomasi, V. Barone, B. Mennucci, M. Cossi, G. Scalmani, N. Rega, G. A. Petersson, H. Nakatsuji, M. Hada, M. Ehara, K. Toyota, R. Fukuda, J. Hasegawa, M. Ishida, T. Nakajima, Y. Honda, O. Kitao, H. Nakai, M. Klene, X. Li, J. E. Knox, H. P. Hratchian, J. B. Cross, V. Bakken, C. Adamo, J. Jaramillo, R. Gomperts, R. E. Stratmann, O. Yazyev, A. J. Austin, R. Cammi, C. Pomelli, J. Ochterski, P. Y. Ayala, K. Morokuma, G. A. Voth, P. Salvador, J. J. Dannenberg, V. G. Zakrzewski, S. Dapprich, A. D. Daniels, M. C. Strain, O. Farkas, D. K. Malick, A. D. Rabuck, K. Raghavachari, J. B. Foresman, J. V. Ortiz, Q. Cui, A. G. Baboul, S. Clifford, J. Cioslowski, B. B. Stefanov, G. Liu, A. Liashenko, P. Piskorz, I. Komaromi, R. L. Martin, D. J. Fox, T. Keith, M. A. Al-Laham, C. Y. Peng, A. Nanayakkara, M. Challacombe, P. M. W. Gill, B. G. Johnson, W. Chen, M. W. Wong, C. Gonzalez and J. A. Pople, *GAUSSIAN 03 (Revision B.05)*, Gaussian, Inc., Wallingford, CT, 2004.
18 E. Castiglioni, F. Lebon, G. Longhi and S. Abbate, *Enantiomer*, 2002, **7**, 161.
19 S. Abbate, E. Castiglioni, F. Gangemi, R. Gangemi, G. Longhi, R. Ruzziconi and S. Spizzichino, *J. Phys. Chem. A*, 2007, **111**, 7031–7040; G. Longhi, S. Abbate, R. Gangemi, E. Giorgio and C. Rosini, *J. Phys. Chem. A*, 2006, **110**, 4958–4968; G. Longhi, R. Gangemi, F. Lebon, E. Castiglioni, S. Abbate, V. M. Pultz and D. A. Lightner, *J. Phys. Chem. A*, 2004, **108**, 5338–5352.
20 C. Guo, R. D. Shah, R. K. Dukor, X. Cao, T. B. Freedman and L. A. Nafie, Enantiomeric Excess Determination by Fourier Transform Near-Infrared Vibrational Circular Dichroism Spectroscopy: Simulation of Real-Time Process Monitoring, *Appl. Spectrosc.*, 2005, **59**, 1114–1124.
21 Y. Nakao, H. Sugeta and Y. Kyogoku, *Chem. Lett.*, 1984, 623–626.
22 C. Sandorfy, *J. Mol. Struct. (THEOCHEM)*, 2002, **614**, 365–366.
23 P. J. Stephens, *J. Phys. Chem.*, 1985, **89**, 748–750.
24 I. M. Mills and A. G. Robiette, *Mol. Phys.*, 1985, **56**, 743–765.
25 V. Barone, *J. Chem. Phys.*, 2005, **122**, 14108.
26 P. L. Polavarapu, *Mol. Phys.*, 1996, **99**, 231.